New scale analyses reveal centenarian African coelacanths

Kelig Mahe, Bruno Ernande, Marc Herbin

New scale analyses reveal centenarian coelacanths *Latimeria chalumnae*

Kélig Mahé[1], Bruno Ernande[2,3], Marc Herbin[4]

1 IFREMER, Fisheries Laboratory, Boulogne sur mer, France.
2, MARBEC, Univ. Montpellier, IFREMER, CNRS, IRD, Montpellier, France
3 Evolution and Ecology Program, International Institute for Applied Systems Analysis (IIASA), Schlossplatz 1, A-2361 Laxenburg, Austria
4 Mécanismes Adaptatifs et Evolution (MECADEV, UMR7179) Muséum national d'histoire naturelle de Paris, CNRS, CP 55, 57 rue Cuvier 75005 Paris, France.

Lead Contact : Kélig Mahé

Summary

The extant coelacanth was discovered in 1938[1]; its biology and ecology remain poorly known due to the low number of specimens collected. Only two previous studies[1,2] have attempted to determine its age and growth. They suggested a maximum lifespan of 20 years placing the coelacanth among the fastest growing marine fish. These findings are at odds with the coelacanth's other known biological features including low oxygen-extraction capacity, slow metabolism, ovoviviparity, and low fecundity, typical of fish with slow life-histories and slow growth. In this study, we use polarized light microscopy to study growth on scales based on a large sample of 27 specimens. Our results demonstrate for the first time nearly imperceptible annual calcified structures (circuli) on the scales and show that maximal age of the coelacanth was underestimated by a factor of 5. Our validation method suggests that circuli are indeed annual thus supporting that the coelacanth is among the longest-living fish species, its lifespan being probably around 100 years. Like deep-sea sharks with a reduced metabolism, the coelacanth has amongst the slowest growth for its size. Further reappraisals of age at first sexual maturity (in the range 40 to 69 years old) and gestation duration (of around 5 years) show that the living coelacanth has one of the slowest life histories of all marine fish and possibly the longest gestation. As long-lived species with slow life histories are

extremely vulnerable to natural and anthropogenic perturbations, our results suggest that coelacanths may be more threatened than previously considered.

Keywords :

Scalimetry, Growth patterns, Polarized light, long-lived species, life-history traits

Results and Discussion

A new ageing methodology

Extant coelacanths were discovered in 1938 and are the only surviving members of an extinct lineage[3]. The coelacanths are large lobe-finned fish (sarcopterygians). The African coelacanth *Latimeria chalumnae*[3,4] is considered critically endangered. This species is characterized by a large body size that can reach up to two meters in length and weigh up to 105 kg[5], with large length at maturity (around 150 cm[6,7]). These animals are ovoviviparous, produce a relatively small number of offspring, and have a large size at birth (around 35 cm). The coelacanth is thought to be a nocturnal languid drift-hunter and its unique locomotory movements are generally slow[8], though it can exhibit fast-start escape responses[9]. These fish have a slow metabolism[10,11] often thought to be associated with its energy-saving mode of life, typical of deep water species. African coelacanths are found most commonly at water temperatures between 15 to 19°C where their oxygen uptake capacity is optimal[10]. These life-history, physiological and behavioural traits initially positioned coelacanths at the slow end of the slow-fast life-history continuum[12]. Growth estimates presented in two previous studies[1,2] using the same dataset of 12 specimens, however, placed coelacanths among the fastest growing fishes, comparable to tunas[13]. The inconsistency between a suggested fast body growth and other life-history traits indicative of slow life-history prompted us to revisit the age and body growth estimations of coelacanths. In this study, age and growth were estimated from scales collected from 27 coelacanths captured of the coast of the Comoros Islands (13

57 females, 11 males, 1 juvenile, and 2 embryos) with total length ranging from 30.5 to 180 cm.
58 These specimens were captured between 1953 and 1991 (See also Table S1). The scales of
59 coelacanths present an anterior field with ridges radiating from the apex and concentric
60 macroscopic circuli[1] (called macro-circuli hereafter) observable under transmitted light
61 microscopy (Figure 1). Both previous ageing studies interpreted these macro-circuli as marks
62 of growth rate variation with alternating translucent and opaque bands suggesting fast and
63 reduced growth, respectively; however, these studies did not agree on the periodicity of band
64 formation. The earliest study suggested that macro-circuli were seasonal with two being laid
65 down each year in association with the alternation of two wet and two dry seasons annually in
66 the tropics[1], whereas the most recent study interpreted macro-circuli as annual, only one being
67 laid down each year[2], arguing that, as for the majority of fish[14], tropical fish exhibit a
68 circannual rhythm despite climate seasonality.

69 Following these earlier studies, we analysed our extended sample under transmitted
70 light microscopy to count the macro-circuli along the longest growth axis of each scale
71 (Figure 1a). The age of the individuals was estimated to range between 0 to 8 years and
72 between 1 to 17 years under the hypothesis that macro-circuli are seasonal and annual,
73 respectively (See also Table S1). These age ranges and the total length range of our sample
74 are comparable to those of the previous ageing studies, thus suggesting an equally fast body
75 growth inconsistent with other life-history traits. We therefore decided to use another
76 observation method, namely polarized-light microscopy. As expected, polarized light revealed
77 much more detail on scale topography than transmitted light[15,16] (Figure 1b), the quality of the
78 image being equivalent to micro-computed tomography (See also Figure S1). More
79 specifically, we identified new circuli that were thinner and more numerous than the macro-
80 circuli observed under transmitted light (Figure 1b vs. Figure 1a). These circuli were also
81 formed by alternating thin translucent and opaque bands suggestive of growth rate variation.

Counting circuli in the same manner as macro-circuli and under the assumption that they are annual, we obtained individual ages ranging from 5 to 84 years (See also Table S1). Comparing our results under transmitted and polarized light, the number of circuli appeared linearly related to the number of macro-circuli (P = 0.009; R^2=0.84) with a slope of 5.16, which indicates the appearance of a macro-circulus roughly every five circuli.

Validation of coelacanth age

Only direct validation methods, i.e., those using individual-level temporal reference marks on scales relative to natural marks to assess the periodicity of the latter, would allow indisputable confirmation of the interpretation of circuli as annual growth marks. The main direct validation methods are (i) mark-recapture of wild individuals tagged externally and labelled with a chemical depositing a mark on their scales and (ii) captive rearing of either chemically-labelled fish of unknown age or of fish of known age (e.g. produced in controlled conditions). These methods are, however, not applicable to coelacanths due to conservation and ethical issues.

Instead, we used indirect validation methods. The most widely used method is Marginal Increment Analysis (MIA), which assesses the periodicity of increments in calcified structures, here macro-circuli and circuli. When growth has a circannual rhythm, increments are formed during the growth period of the year. The size of the increment under formation, named the marginal increment and measured as the distance between the last fully formed (macro-) circulus and the edge of the scale, should thus exhibit some intra-annual periodic pattern when plotted against the month at which the individual was captured. Applying MIA to macro-circuli, no such intra-annual periodic pattern was evident (P = 0.61; Figure 1 lower panel) suggesting that they are not formed annually. In contrast, the application of MIA to circuli allowed detection of intra-annual variation in their growth (P < 0.001; Figure 1 upper panel), revealing a circannual rhythm in circuli formation.

A second indirect validation method is to assess the internal and/or external consistency of the population-level mean body growth pattern, or length-at-age data, obtained for each scale. Three growth models are widely used in ecology to describe length-at-age data for species with indeterminate growth because they conform to the observed shape of growth curves: the von Bertalanffy, Gompertz, and logistic growth models. For both macro-circuli and circuli ageing, the von Bertalanffy growth model appeared to best described the resulting length-at-age data based on minimization of the small-sample bias-corrected AIC (See also Table S2). The body growth curve estimated from length-at-age data obtained using macro-circuli for ageing (Figure 2 dashed blue curve) was characterized by a combination of a large asymptotic length ($TL_\infty = 296.1$ cm) reached at a fast rate ($K = 0.05\ \text{year}^{-1}$; note that coefficient K in the von Bertalanffy model represents the rate at which asymptotic length is reached and not size change per unit of time). Consequently, the largest ($TL = 180$ cm) and oldest (17 years) specimen of our sample appeared as being still in a fast growth phase and at about only 61% of the estimated asymptotic length TL_∞. Moreover, TL_∞ was estimated to be much larger than both the largest individual ever captured[17] ($TL = 190$ cm) and the maximum length ($TL_{\max} \pm \text{c.i.} = 199 \pm 24$ cm) estimated independently from length-at-age data using extreme value theory[2]. The same holds when using length-at-age data obtained by the previous ageing study assuming annual macro-circuli (Figure 2 dashed dark blue curve). In contrast, the body growth model fitted to length-at-age data obtained using circuli (Figure 2 red curve) estimated a smaller asymptotic length ($TL_\infty = 203.8$ cm) reached at a slower rate ($K = 0.02\ \text{year}^{-1}$) such that the largest ($TL = 180$ cm) and oldest (85 years) individual in the data set is in a slow growth phase and much closer to its asymptotic length (88%). In addition, TL_∞ is in much better agreement with the length of the largest individual ever captured and with the previously independently estimated maximum length. The growth pattern obtained using circuli ageing appears thus to outperform other estimates.

We further used a double logarithmic plot of the von Bertalanffy rate coefficient K versus asymptotic length TL_{∞} (so-called auximetric plot), and the growth performance index ϕ' to compare the global body growth of coelacanths with other marine fish species (1383 populations distributed across 1313 species extracted from FishBase[18]) for each ageing method. Ageing based on macro-circuli would position the coelacanth among the fastest growing fishes with a similar asymptotic length (Figure 3A) and above the 90th percentile of the growth performance index ϕ' distribution across all marine fish (Figure 3B). Such high body growth capacity is almost equivalent to that of tunas[13] (Figure 3) that have evolved unique morphological: streamlined body and fin shapes, large mass-specific gill surface area, and physiological: high oxygen-affinity blood, combined with endothermy, high proportion of red muscle, high cardiac performance[13], characteristics to support their high growth performance and very active lifestyle. These traits differ strongly from those of coelacanths, which are typical of fish with low growth performance and high longevity[19] like deep-sea fish with low metabolic rates. In contrast, the body growth pattern obtained from circuli would place *L. chalumnae* among the slowest growing fish within the same range of asymptotic length (Figure 3A) and close to the mode of the growth performance index ϕ' distribution (64th percentile, Figure 3B). This growth is similar to that of deep-sea sharks, concurring with the morphological and physiological traits of the living coelacanth, as well as its lifestyle.

These results suggest that ageing coelacanths by interpreting circuli as annual growth marks provides the most realistic estimates of seasonal scale formation and lifelong body growth, with the longevity of the coelacanth estimated to be close to one century. This observed longevity is five times greater than previously estimated. Only one study had hypothesised such an extended lifespan[6] but with no direct evidence. Our study unequivocally demonstrates for the first time the coelacanth exceptional longevity and positions it as one of the most long-lived fish species. The factor of five between longevity estimates originates

157 from the fact that the macro-circuli used by the previous studies for ageing do not exhibit a
158 circannual formation rhythm and appear with an approximately 5-year periodicity throughout
159 the lifespan of both males and females (See also Figure S2). Two hypotheses may explain the
160 presence of these macro-circuli, the first one being of exogenous origin, namely periodic
161 environmental events, and the other of endogenous origin, i.e. periodic
162 physiological/behavioural events. Regarding the former, strong variations in environmental
163 conditions such as salinity or temperature are known to leave marks on scales and large-scale
164 climate oscillations such as the Indian Ocean Dipole (IOD) or the El Niño-Southern
165 Oscillation (ENSO)[20] could produce periodic scale marks. However, an exogenous origin
166 would imply a mark deposition on scales that is synchronized across individuals. This
167 synchrony is not observed in the years of appearance of the macro-circuli for the different
168 individuals in our sample (See also Figure S2A). The hypothesis of an endogenous origin
169 (periodic physiological or behavioural stresses) seems thus more likely. Periodic events that
170 affect both sexes equally, as macro-circuli are found in both females and males, such as
171 migration or reproductive behaviour are potential candidates. Unfortunately, knowledge on
172 the biology and behaviour of the coelacanth remains too fragmented to address this hypothesis
173 further.

174 ## Implications for life history and conservation

175 In addition to longevity and body growth, two other aspects the coelacanth's life-history can
176 be reappraised with our new age estimation method: the duration of gestation and the age at
177 first sexual maturity. The early life of coelacanth is not well known and developmental stages
178 available in collections are rare. In our sample, two different *pre-partum* embryos (CCC29.5
179 and CCC162.21), one early *post-partum* juvenile (CCC94), and another slightly older juvenile
180 were available (See also Table S1). The age of both *pre-partum* specimens is estimated at 5
181 years based on circuli whereas that of the two *post-partum* individuals is estimated at 9 and 12

182 years, respectively. This indicates that the gestation duration is at least five years contrary to
183 the 1 to 2 years suggested by earlier studies. The length at birth is uncertain but the size of the
184 largest observed *pre-partum* individual from a litter of 26 near-term embryos[21] ranging from
185 30.8 to 35.8 cm total length found in a gravid female could be a good estimation. Based on
186 our estimate of the von Bertalanffy growth model and under the assumption that embryos
187 follow the same growth pattern as post-partum individuals, such length at birth would also
188 give a gestation period close to five years. The earlier hypothesis of a long gestation is thus
189 confirmed[2] but largely extended, placing the coelacanth among the vertebrates with the
190 longest gestation period, alongside the deep-sea frilled shark *Chlamydoselachus anguineus*
191 (three years)[22].

192 The length at first sexual maturity was estimated to range between 120 and 129 cm for
193 males and between 160 to 179 cm for females[6,7]. These values were obtained from the
194 anatomical and morphological differences between juveniles and matures specimens. In light
195 of our ageing data (See also Table S1), these length ranges would correspond to ages at first
196 maturity ranging from 40 to 69 years for males and from 58 to 66 years for females. These
197 new estimates of age at first maturity are also close to those of the frilled shark and
198 correspond to an onset of maturation much later in life (ratio of age maturity to maximum
199 longevity: 0.47-0.81 for males and 0.68-0.78 for females) than in teleost fishes (range: 0.16-
200 0.39 and typical values: 0.25-0.30[23]). This pattern is consistent with the reproductive strategy
201 of both coelacanth and elasmobranches[24]. Species that rely on internal fertilization and
202 produce a few large fully-developed offspring after a long gestation, especially ovoviviparous
203 and viviparous ones, tend to mature later in life than species that lay very large number of
204 eggs, rely on external fertilization and produce undeveloped larvae (most teleost fishes[25]).
205 This conforms to life-history theory which predicts that an increased survival probability of
206 immature life-stages, such as in case of ovoviviparity and viviparity, favours the evolution of

delayed maturation[26]. The delayed maturity of the coelacanth relative to its longevity also implies a shorter relative reproductive lifespan than teleost fishes. This results in very different benefits and demographic consequences of extreme longevity. In teleost, long-lived species have an extended reproductive lifespan and thus "sample" multiple reproductive events. In a variable environment resulting in fluctuating recruitment, this allows taking advantage of occasional favourable environmental conditions to produce strong year classes literally "stored" in the adult population until conditions for strong recruitment return, a type of bet-hedging strategy also called "storage effect"[27]. In contrast, the coelacanth demography is likely to rely on a continuous influx of weak recruitment insured by very high survival rates of a few offspring per individual whatever the environmental conditions.

Based on our re-appraisal of time-related life-history traits of the coelacanth, namely growth rate through the von Bertalanffy rate coefficient K, maximum observed longevity, age at first sexual maturity and gestation duration, we assessed its location along the slow-fast life-history continuum in marine fish. A Principal Component Analysis was performed on these four life-history traits across 147 populations in 131 marine fish species extracted from FishBase[18]. By focusing on life-history traits with time dimensionality, we avoided the problem of heterogeneous dimensions across traits that may prevent correct interpretation of life-history strategies in terms of the slow-fast continuum[12]. Ideally, the phylogenetic relatedness between species should have been accounted for in this analysis. However, as far as we are aware, no phylogeny relating the coelacanth, Actinopterygii and Chondrichthyes with a sufficiently fine granularity, i.e. including most species of our life-history dataset, is currently available. In addition, past analyses in other taxa have shown that phylogenetic inertia does not affect strongly the detection and strength of the slow-fast continuum[12]. The first Principal Component observed trades-off high longevity and late maturity against fast rate of approach towards asymptotic size, and thus can be considered as the main component

of the slow-fast life-history continuum, whereas the second one is mostly determined by gestation duration (inversely related to spawning frequency used in the analysis; Figure 4A). The estimation of life-history traits based on macro-circuli ageing places the coelacanth in the main bulk of marine fish, close to the cluster formed by tunas (Figure 4A). In contrast, life-history traits estimated from circuli position the coelacanth towards very slow life-histories, close to deep-sea sharks and roughies (Figure 4A). Taking the first PC as a metric of the slow-fast life-history continuum, ageing based on circuli places the coelacanth among the slowest life-histories (0^{th} percentile) together with roughies and deep-sea sharks whereas ageing based on macro-circuli would correspond to a faster, moderate pace of life (26^{th} and 13^{th} percentile for macro-circuli ageing of our data and previous data, respectively; Figure 4B).

The new ageing method developed in this study shows that the African coealacanth, *L. chalumnae,* may live for about a century, making it one of the most long-lived fish species. Alongside its exceptional longevity, this study showed that the African coelacanth has one of the slowest life histories among marine fish, and possibly all vertebrates, characterized by a slow body growth relative to its size, very late age at first sexual maturity, and exceptionally long gestation time, which is in concord with its ovoviviparity, relatively small clutch size, and reduced metabolism. These life-history and physiological characteristics are partly similar to those observed in the human fish (*Proteus anguinus*)[28], a small cave salamander with one of the slowest life-histories among vertebrates. Long-lived species characterized by slow life history and relatively low fecundity are known to be extremely vulnerable to perturbations of a natural or anthropic nature due to their very low replacement rate[29]. Ignoring such characteristics has been shown to be detrimental to conservation and management as exemplified by some deep-sea fisheries[30]. The African coelacanth is assessed as critically endangered (Red List of Threatened Species of IUCN). Our results suggest that it may be even more threatened than expected due to its peculiar life history. Further studies on the

biology and ecology of the coelacanth, especially on its reproductive biology and behaviour, are needed to be able to preserve this unique component of life on Earth.

Acknowledgements

We are grateful to R. Elleboode and G. Bled Defruit for age readings. We thank C. Bens and A. Verguin of the Collection de Pièces anatomiques en Fluides at the Muséum National d'Histoire Naturelle (MNHN) for their help, E. Sultan of UMR LOCEAN CNRS-MNHN for providing the Comoros climatic data, and L. Poloni, S. Couette and C. Toti Lutet for micro-computed tomography scanning of scales of one specimen at MorphOptics of the UMR CNRS uB EPHE 6282 Biogéosciences. We would especially thank M. Etherton, W. McCurdy, A. Herrel and K. M. MacKenzie for their valuable help in editing this manuscript. We are extremely grateful to the two anonymous referees, J.M. Gaillard and the Editor for their especially helpful and constructive comments to improve the manuscript. The MNHN gives access to its collections in the framework of the RECOLNAT national Research Infrastructure.

Author contributions

M.H., K.M. and B.E. contributed conception and design of the study. M.H. performed the sampling. K.M. organized the image acquisition and ageing data collection. K.M.. performed the analysis of growth patterns and the marginal increment analysis and B.E. the auximetric analysis and the slow-fast life-history continuum analysis. All authors provided inputs for the results and discussion. K.M. wrote the first draft of the manuscript and B.E. wrote sections of the manuscript. All authors provided critical comments and were involved in the revision and editing of the manuscript. All authors accepted the final version of the manuscript.

Declaration of interests

The authors declare no competing interests.

Figure Legends

Figure 1: Analysis and periodicity of the circuli and macro-circuli of the African coelacanth scale. The same scale of *L. chalumnae* CCC4 (female of 109 cm caught in January 1954) is analysed based on a reconstructed image under either transmitted light microscopy (a.) or polarized light microscopy (b.) (Horizontal white scale bar = 1 mm). Macro-circuli (a.) and circuli (b.) are marked (dots) along the longest growth axis (red line). For each type of circuli, temporal dynamics of monthly marginal increments (mm) on scales of *L. chalumnae* (n = 27) based on the hypothesis of annual circuli (red) or annual macro-circuli (blue) are shown. The bottom and top of each box are the first and the third quartiles of the marginal increment distribution for the considered month (x-axis), the horizontal segment and the diamond inside the box are respectively the median and the mean, and whiskers represent the most extreme data point within 1.5 interquartile range. For three specimens (CCC162.21, CCC29.5 and CCC42.5), only macro-circuli could be identified and no individual was collected in November and December so that no marginal increment was available for month 10 and 12. The thin continuous curve in each panel represents the fit of a sinusoidal regression of marginal increments against month with a period of 12 month to test for annual periodicity. Under the hypothesis of annual circuli, a significant intra-annual periodicity of marginal increment growth is detected by the sinusoidal regression. In contrast, under the assumption of annual macro-circuli, no evidence of a periodic pattern is found (See also Figure S1 and S2).

Figure 2: Body growth pattern of the African coelacanth according to different scale interpretations. Observed length-at-age data for different scale interpretations for age are shown (red solid circles: circuli ageing, blue open squares: macro-circuli ageing, dark blue crosses: previous age interpretation[2]) together with the corresponding fitted von Bertalanffy growth models (dashed light blue curve: macro-circuli, continuous red curve: circuli, dashed dark blue curve: previous age interpretation). TL_∞ and K are the asymptotic total length (cm) and the rate coefficient, i.e. the rate at which the asymptotic lentgh is reached (year^{-1}), respectively, estimated from the von Bertalanffy growth models and $\phi' = \log(K) + 2\log(TL_\infty)$ is the growth performance index (cm.year^{-1}) that allows overall growth performance comparison across populations or species. The grey area represents embryos *in utero*. The black horizontal line indicates the size of the largest specimen ever captured (See also Table S1 and S2).

Figure 3: Comparison of the African coelacanth growth rate characteristics to other marine fish under the various ageing hypotheses. A. Auximetric plot of the coelacanth under the various ageing hypotheses (red diamond: annual circuli, light blue diamond: annual macro-circuli from present study; dark blue diamond: annual macro-circuli from previous study) relative to other taxonomic groups of marine fish species (solid circles; orange: tunas; purple: deep-sea sharks; green: roughies; grey: other fish species). The auximetric plane is the plane defined by two logarithmic axes representing the von Bertalanffy rate coefficient K versus asymptotic total length TL_∞ where a population characterized by a set of von Bertalanffy growth parameters (TL_∞, K) is represented by a point. Populations of a given species or species having similar growth characteristics will tend to form clusters of points that delimit the growth space of that species or group of species. 95% ellipses, i.e. contours enclosing 95% of the data points under the assumption of a bivariate-normal distribution, are drawn to illustrate the growth space of tunas (orange circle), deep-sea sharks (purple circle) and roughies (green circle) for better comparison. The auximetric plot allows comparison of species according to their speed of growth at a given asymptotic size (vertical direction) and according to their body size for a given speed of growth (horizontal direction). It also allows comparison of species in terms of their global growth capacity by superimposing isolines of the growth performance index $\phi' = \log(K) + 2\log(TL_\infty)$ since these have a known slope of 2 (dashed black lines labelled with the corresponding ϕ' value). **B**. Growth performance index $\phi' = \log(K) + 2\log(TL_\infty)$ of the coelacanth (diamonds) under the various ageing hypotheses (same colors as in A) relative to other taxonomic groups of marine fish species (boxplots; same colors as in A). Labelled vertical lines give the percentiles of the distribution of ϕ' values across all marine fish species corresponding to the ϕ' values of the African coelacanth under the various ageing hypotheses. Boxplots are defined as in Figure 1. Von

344 Bertalanffy growth parameters for other marine fish were extracted from FishBase in June
345 2020 (1383 populations distributed across 1313 species).

346

347 **Figure 4: Locating the African coelacanth along the slow-fast life-history continuum in**
348 **marine fish under the various ageing hypotheses**. **A.** Biplot of the two first axes of a
349 Principal Component (PC) analysis on time-related life-history traits (von Bertalanffy rate
350 coefficient K, sexual maturity age, maximum observed longevity and spawning
351 frequency/inverse of gestation time) of marine fish after log10-transformation, removal of the
352 effect of body size, centering and scaling. The coelacanth projection (diamonds) on the PC
353 plane under the various ageing hypotheses (same colors as in Figure 3) can be compared to
354 the projections of other taxonomic groups of marine fish species (solid circles; same colors as
355 in Figure 3). The percentage of variance explained by the PCs is indicated between
356 parentheses in axis labels. Arrows indicate how much each life-history trait contributes to
357 each PC according to its projection on each PC axis and the angle between the arrows is
358 indicative of the correlation between life-history-traits, orthogonality meaning independence
359 and opposite directions meaning negative correlations. Clearly, the first PC corresponds to the
360 slow-fast life-history continuum as it trades-off high longevity and late maturation on the left
361 hand side against fast approach rate towards asymptotic length on the right hand side whereas
362 the second PC mainly involves spawning frequency. **B.** Position of the coelacanth (diamonds)
363 under various ageing hypotheses (same colors as in Figure 3) relative to other taxonomic
364 groups of marine fish species (boxplots; same colors as in Figure 3) along the slow-fast life-
365 history continuum (scores along PC1, panel A). Labelled vertical lines give the percentiles of
366 the distribution of the scores along PC1 of all marine fish species that correspond to the scores
367 of the coelacanth under the various ageing hypotheses. Boxplots are defined as in Figure 1.

Life-history traits for other marine fish were extracted from FishBase in June 2020 (147 populations distributed across 131 species).

STAR METHODS

RESOURCE AVAILABILITY

Lead contact

Further information and requests for resources should be directed to and will be fulfilled by the Lead Contact, Kélig MAHE (kelig.mahe@ifremer.fr)

Materials availability

This study did not generate any reagents or other materials.

Data and code availability

All data on coelacanth specimens are available in the Supplementary Material. Data on the other marine fish species were extracted from FishBase in June 2020 (see Key resources table). All data extracted and R codes supporting the current study have been deposited in SEANOE (https://doi.org/10.17882/80498).

EXPERIMENTAL MODEL AND SUBJECT DETAILS

Between 2 and 5 scales were sampled from the basal part of the first dorsal fin of coelacanth specimens from public natural history collections: two specimens of the Zoologischen Staatssammlung München (ZSM; The Bavarian State Collection of Zoology) and 25 of the Collections des pieces anatomiques en fluide from the Muséum National d'Histoire Naturelle de Paris (MNHN; The French National Museum of Natural History). For each specimen, we provide its inventory number of the institution that houses the collection and the Coelacanth Conservation Council (CCC) number[17] (See also Table S1). The specimens of the MNHN and ZSM are stored in 10% formalin and 70° alcohol, respectively. The MNHN's specimens are

conserved in the formalin since their capture and, with time, the un-buffered conservative solution became acid, which could have damaged the structure of some scales.

METHOD DETAILS

Sclerochronology

The coelacanth has an elasmoid-type scale that has evolved several times independently in the evolutionary history of fish. All scales were rehydrated and cleaned. After this preliminary step, they were photographed under transmitted light using a Zeiss microscope equipped with a camera to observe the series of concentric macroscopic circuli (macro-circuli). In a second step, they were photographed under polarized light microscopy in order to increase the contrast between structures. Polarized light microscopy reveals topographical details on anisotropic materials, including bio-calcified structures such as scales, which are difficult to observe under transmitted light. Polarized light revealed more numerous circuli, thinner than the macro-circuli and formed by alternating translucent and opaque bands suggestive of growth rate variation. Several scales were scanned using a micro-computed tomography scanner (CT scan) providing a high resolution 3-dimensional representation of the object. In a few cases, the structures on the scale were not distinguishable due to degradation by the formalin solution and thus scale interpretation was not possible in the corresponding specimens (See also Table S1).

The image processing was performed using the image analysis system TNPC (Digital processing for calcified structures) for pictures under both transmitted and polarized light. Two sclerochronology experts analyzed each scale by identifying macro-circuli under transmitted light and circuli under polarized light along the longest growth axis, i.e. from the proximal to the distal end of the scale (Figure 1). Several scales per specimen were used to obtain a robust estimate of the number of (macro-) circuli and thus of the age of the specimen under the assumption of an annual growth periodicity (see age validation method below).

Age validation method: Marginal Increment Analysis

Calcified structures in fish have the potential to grow throughout the life of the individual without resorption. Variations in the individual's body growth are translated into variations in the growth of the calcified structures. These variations are revealed by the optical properties of the bio-calcified material that appears either opaque or translucent. Hence, circannual rhythm in body growth and calcified structure formation produces an alternation of translucent and opaque bands on the latter. Pairs of translucent-opaque bands correspond to annual increments and can thus be used for ageing individuals. However, for using observed increments on calcified structures (here macro-circuli and circuli on coelacanth scales) to age individuals, it is necessary to validate their annual frequency of formation as any event affecting growth may produce such a mark (e.g. transition from endogenous to exogenous nutrition in larvae, migration, gestation, thermal shock). Such age validation is required for establishing the accuracy of an age estimation method[31].

Marginal Increment Analysis (MIA) is the most commonly used age validation method and allows assessing the periodicity of increment formation in bio-calcified structures[32]. It is a quantitative approach that relies on a measure of the size of the increment under formation (named the marginal increment), i.e., the distance between the most recently formed (macro-) circuli and the edge of the scale, relative to the size of the last fully formed increment, i.e., the distance between the last-but-one and the most recently formed (macro-) circuli. In mathematical notation, the relative measure of the marginal increment, MI, is given by:

$$\mathrm{MI} = \frac{R_O - R_n}{R_n - R_{n-1}}$$

Where R_O is the radius of the scale measured from its focus to the edge (Figure 1), R_n is the distance between the focus and the last (macro-) circuli formed n, and R_{n-1} is the distance between the focus and the last-but-one (macro-) circuli $n-1$. If (macro-) circuli are formed

annually, the marginal increment MI will thus exhibit an intra-annual periodic pattern that can be observed by plotting its measure against the date of its origin, i.e. the month at which the specimen was captured. MI was measured for each specimen using macro-circuli under transmitted light and circuli under polarized light and plotted against the month of capture. A sinusoidal regression of MI against the month of capture m with a period of 12 months was used to test for the annual periodicity of (macro-)-circuli formation after linearization:

$$\mathrm{MI}\sim a + b\sin\left(\frac{2\pi}{12}m + c\right) = a + b\sin(c)\cos\left(\frac{2\pi}{12}m\right) + b\cos(c)\sin\left(\frac{2\pi}{12}m\right) \quad (1a)$$

so that,

$$\mathrm{MI}\sim\alpha_0 + \alpha_1\cos\left(\frac{2\pi}{12}m\right) + \alpha_2\sin\left(\frac{2\pi}{12}m\right) \quad (1b)$$

with $a = \alpha_0$, $b = (\alpha_1^2 + \alpha_2^2)^{1/2}$, and $c = \arctan(\frac{\alpha_1}{\alpha_2})$.

The global significance of the linear regression provided a statistical validation for an intra-annual pattern in (macro-) circuli MI. The classical assumptions of the linear models (normality of, homoscedasticity of, and absence of trends in the residuals) were verified and met.

Body growth models

The mean body growth patterns of the sampled specimens obtained by interpreting scales using macro-circuli and circuli were described using three different growth models including:

a) the von Bertalanffy[33] model:

$$TL_t = TL_\infty - (TL_\infty - TL_1).e^{-K.(t-1)} \quad (2)$$

b) the Gompertz[34] model:

$$TL_t = TL_\infty.e^{\ln\left({}^{TL_1}/_{TL_\infty}\right)..e^{-K.(t-1)}} \quad (3)$$

c) the logistic model[35]:

$$TL_t = \frac{\mathrm{TL}_\infty}{1+\left(\left(\frac{\mathrm{TL}_\infty}{TL_1}\right)-1\right)*e^{-K.(t-1)}} \quad (4)$$

Where TL_1, TL_t, and TL_∞ are respectively the length at age 1, at age t and the asymptotic length, and K is the rate at which the asymptote is reached, called the rate coefficient is this paper. Notice that the models started at age 1 as no data was available for age 0 individuals, hence the age offset of 1 in the exponential: $t-1$.

Auximetric plot and growth performance comparison

The body growth patterns obtained for coelacanth macro-circuli and circuli were compared with those of other marine species using two complementary approaches.

First, an auximetric plot[36], which is a double logarithmic plot (base 10) of the von Bertalanffy growth model parameters K versus TL_∞, was produced. Given that K represents the rate at which TL_∞ is reached in inverse time units whereas TL_∞ represents the size range of the species in size units, it is difficult to compare multiple growth patterns while accounting for both dimensions at the same time. In addition, the fact that K and TL_∞ are negatively correlated complicates the matter. The auximetric plot allows circumventing these difficulties. A population characterized by a set of von Bertalanffy growth parameters (TL_∞, K) is represented by a point and populations of a given species or species having similar growth characteristics will tend to form clusters of points that delimit the growth space of that species or group of species. Moreover, the auximetric plot allows the comparison of species according to their speed of growth at a given asymptotic size (vertical direction) and according to their body size for a given speed of growth (horizontal direction).

Second, the "growth performance index"[36] was computed:

$$\phi' = \log_{10} K + 2\log_{10} TL_\infty \quad (5)$$

This index has the interesting property of having the same dimension as a growth rate, i.e. size per unit time, and thus allows to compare the global growth performances across species. A

very high growth index would correspond to species growing fast to large sizes relative to species with a low one. Empirically, the index ϕ' is shown to be distributed normally for populations of the same species or phylogenetically close species. Isolines of the index ϕ' can be superimposed to the auximetric plot since these have a known slope of 2, thus allowing both approaches to be used at the same time.

Both approaches were used for the comparison of the coelacanth with other marine fish species. Von Bertalanffy parameters for the other marine fish species were extracted from FishBase in June 2020 (Popgrowth table[18]). Only populations for which size was measured as total length were kept for comparison, resulting in 1383 populations distributed across 1313 species.

Slow-fast life-history continuum analysis

The location of the coelacanth along the slow-fast life-history continuum[12] in marine fish was assessed using estimates of time-related life-history traits obtained from both macro-circuli and circuli ageing: the von Bertalanffy rate coefficient K (yr^{-1}), the maximum observed longevity (yr), the age at first sexual maturity (yr), and the gestation duration (yr) transformed into a spawning frequency (yr^{-1}). These four traits were extracted for other marine fish species from FishBase in June 2020 (Popgrowth, Species, Maturity, Fecundity and Spawning tables[18]) and were available together for 147 populations distributed across 131 species.

QUANTIFICATION AND STATISTICAL ANALYSIS

Body growth models

For both macro-circuli and circuli ageing, the best growth model was identified as the one minimizing the small-sample, bias-corrected form of the Akaike Information Criterion (AICc[37,38]). The AICc balances the trade-off between the quality of fit and the number of parameters used[38] while accounting for small-sample bias and is defined as:

$$\mathrm{AICc} = 2k - 2\ln(L) + \frac{2k(k+1)}{n-k-1} \quad (6)$$

where n is the sample size, k is the total number of parameters of the model and L is its likelihood.

Slow-fast life-history continuum analysis

As time-related life-history traits are known to be affected by body size[12], the four traits were regressed against asymptotic total length TL_∞ after log10-transformation of the five variables. A Principal Components (PC) analysis was then carried out on the residuals of the regressions of the four life-history traits after centering and scaling. The two first PCs explained 78.9% of the variation. A biplot on the plane defined by the two first PCs was produced in order to identify the slow-fast life-history continuum and to position the coelacanth life-history as estimated by the two ageing methods. The biplot represents both populations' projection on the PC plane as dots and life-history trait projection as arrows.

Statistical analyses and plots were performed using the following packages in the statistical environment R: Rfishbase[39], ade4[40], ggplot2[41], factoextra[42], ggpubr[43].

ADDITIONAL RESOURCES

References

1. Hureau, J. C. and Ozouf, C. (1977). Determination de l'âge et croissance du coelacanthe *Latimeria Smith*, 1939 (poisson, crossopterygian, coelacanthide). Cybium. Ser. *3*, 129–137.

2. Froese, R., and Palomares, M.L.D. (2000). Growth, natural mortality, length weight relationship, maximum length and length-at-first-maturity of the coelacanth *Latimeria*. Environ. Biol. Fish *58*, 45–52. https://doi.org/10.1023/A:1007602613607.

3. Smith, J.L.B. (1939). A living fish of Mesozoic type. Nature *143*, 455–456. https://doi.org/10.1038/143455a.

539 4. Fricke, H. Hissmann, K., Schauer, J., Reinicke, O., and Ksang, L. (1991). Habitat and
540 population size of the coelacanth *Latimeria chalumnae* at Grand Comoro. Environmental
541 Biology Fishes. *32*, 287–300. https://doi.org/10.1007/BF00007462

542 5. Smith, C. L., Rand, C. S., Schaeffer, B., and Atz. J.W. (1975). *Latimeria*, the living
543 coelacanth, is ovoviviparous. Science *190*, 1105–1106.
544 https://doi.org/10.1126/science.190.4219.1105

545 6. Fricke, H., Hissmann, K., Froese, R., Schauer, J., Plante, R., and Fricke, S. (2011). The
546 population biology of the living coelacanth studied over 21 years. Mar. Biol. *158(7),* 1511-
547 1522. https://doi.org/10.1007/s00227-011-1667-x.

548 7. Bruton, M. N., and Armstrong, M. J. (1991). The demography of the coelacanth *Latimeria*
549 *chalumnae*. Environ. Biol. Fish. *32*, 301–311. https://doi.org/10.1007/BF00007463.

550 8. Hismann, K., Fricke H., and Schauer. J. (2000). Patterns of time and space utilisation in
551 coelacanths (*Latimeria chalumnae*), determined by ultrasonic telemetry. Mar. Biol. *136*, 943-
552 952. https://doi.org/10.1007/s002270000294.

553 9. Décamps, T., Herrel, A., Ballesta, L., Holon, F., Rauby, T., Gentil, Y., Gentil, C., Dutel, H.,
554 Debruyne, R., Charrassin, J.-B., *et al.* (2016). The third dimension: a novel set-up for filming
555 coelacanths in their natural environment. Methods in Ecol. Evol. *8*: 322-328.
556 https://doi.org/10.1111/2041-210X.12671.

557 10. Hughes, G.M. (1995). The gills of the coelacanth, *Latimeria chalumnae*, a study in
558 relation to body size. Philosophical Transactions of the Royal Society of London B. *347*, 427-
559 438. https://doi.org/10.1098/rstb.1995.0034.

560 11. Fricke, H., and Hissman, K. (2000).Feeding ecology and evolutionary survival of the
561 living coelacanth *Latimeria chalumnae*. Mar. Biol. *136,* 379-386.
562 https://doi.org/10.1007/s002270050697.

12. Gaillard, J. M., Lemaître, J. F., Berger, V., Bonenfant, C., Devillard, S., Douhard, M., Gamelon, M., Plard, F., and Lebreton, J. D. (2016) Life history axes of variation. In The Encyclopedia of Evolutionary Biology, R. Kliman, ed. (Cambridge : Academic Press), pp. 312–323.

13. Murua, H. Rodriguez-Marin, E. Neilson, J. D. Farley, J. H., and Juan-Jordá, M. J. (2017). Fast versus slow growing tuna species: age, growth, and implications for population dynamics and fisheries management, Rev. Fish Biol. Fisher. *27(4),* 733-773. https://doi.org/10.1007/s11160-017-9474-1.

14. Vitale, F., Worsøe Clausen, L., and Ní Chonchúir, G. (2019). Handbook of fish age estimation protocols and validation methods. ICES Coop. Res. Rep. *346*, 1-180 http://doi.org/10.17895/ices.pub.5221.

15. Treble, M. A., Campana, S. E., Wastle, R. J., Jones, C. M., and Boje, J. (2008). Growth analysis and age validation of a deepwater Arctic fish: the Greenland Halibut (*Reinhardtius hippoglossoides*). Can. J. Fish. Aquat. Sci. *65*, 1047–1059. https://doi.org/10.1139/F08-030.

16. Le Cren, E. D. (1947).The determination of the age and growth of the perch (*Perca fluviatilis*) from the opercular bone. J. Anim**.** Ecol. *16*, 188 – 204. https://doi.org/10.2307/1494.

17. Nulens, R., Scott, L., and Herbin, M. (2011).An updated inventory of all known specimens of the coelacanth, *Latimeria* spp. Smithiana Special Publication *3*, 1–52.

18. Froese, R., and Pauly. D. Editors. FishBase. World Wide Web electronic publication. www.fishbase.org (12/2019)

19. Cailliet, G. M., Andrews, A.H., Burton, E.J., Watters, D.L., Kline, D.E., and Ferry-Graham, L.A. (2001). Age determination and validation studies of marine fishes: do deep-

587 dwellers live longer, Exper. Gero. *36*, 739-764. https://doi.org/10.1016/S0531-
588 5565(00)00239-4.
589 20. Sinha, M., Jha, S., and Chakraborty, P., (2020).Indian Ocean wind speed variability and
590 global teleconnection patterns. Oceanologia, Preprint at
591 https://doi.org/10.1016/j.oceano.2019.10.002.
592 21. Heemstra, P.C., and Greenwood. P.H. (1992). New observations on the visceral anatomy
593 of the late term foetuses of the living coelacanth fish and the oophagy controversy.
594 Proceeding of the Royal Society of London B. *249*, 49-55.
595 https://doi.org/10.1098/rspb.1992.0082.

596 22. Tanaka, S., Shiobara, Y., Hioki, S., Abe, H., Nishi, G., Yano, K., and Suzuki, K., (1990).
597 The reproductive biology of the frilled shark, *Chlamydoselachus anguineus* from Suruga Bay,
598 Japan. Jap. J. Ichthyol**.** *37(3),* 273-291. https://doi.org/10.11369/jji1950.37.273.
599 23. Beverton, R. J. H. (1992). Patterns of reproductive strategy parameters in some marine
600 teleost fishes. J. Fish Biol. *41(sB),* 137–160. https://doi.org/10.1111/j.1095-
601 8649.1992.tb03875.x

602 24. Conrath, C. L., and Musick, J. A. (2012). Reproductive Biology of Elasmobranchs. In
603 Biology of Sharks and Their Relatives, J.C. Carrier, J.A. Musick, and M.R. Heithaus, eds.
604 (Floride : CRC Press), pp. 307–328.

605 25 Gunderson, D. R. (1997). Trade-off between reproductive effort and adult survival in
606 oviparous and viviparous fishes. Can. J. Fish. Aquat. Sci. *54(9),* 990-998.

607 26 Ernande, B., Dieckmann, U., and Heino, M. (2004). Adaptive changes in harvested
608 populations: Plasticity and evolution of age and size at maturation. Proceedings of the Royal
609 Society of London Series B *271*, 415–423.

610 27 Warner, R. R., and Chesson, P. L. (1985). Coexistence Mediated by Recruitment
611 Fluctuations: A Field Guide to the Storage Effect. The American Naturalist, *125(6),* 769–787.
612 https://doi.org/10.1086/284379

613 28. Voituron, Y., de Fraipont, M., Issartel, J., Guillaume, O., and Clobert, J. (2011).
614 Evolutionary biology Extreme lifespan of the human fish (*Proteus anguinus*): a challenge for
615 ageing mechanisms. Biol. Lett. *7***,** 105–107. https://doi:10.1098/rsbl.2010.0539.

616 29. Cheung, W.W.L., Pitcher, T.J., and Pauly, D. (2005) A fuzzy logic expert system to
617 estimate intrinsic extinction vulnerabilities of marine fishes to fishing. Biological
618 Conservation, *124*, 97–111. https://doi.org/10.1016/j.biocon.2005.01.017.

619 30. Norse, E. A., Brooke, S., Cheung, W. W. L., Clark, M. R., Ekeland, I., Froese, R., Gjerde,
620 K. M., Haedrich, R. L., Heppell, S. S., Morato, T., *et al.* (2012). Sustainability of deep-sea
621 fisheries. Marine Policy, *36(2)*, 307–320. https://doi.org/10.1016/j.marpol.2011.06.008

622 31. Beamish, R. J., and McFarlane, G. A. (1983). The forgotten requirement for age validation
623 in fisheries biology. Trans. Am. Fish. Soc. *112*, 735–743. https://doi.org/10.1577/1548-8659.
624 32. Campana, S. (2001). Accuracy, precision and quality control in age determination,
625 including a review of the use and abuse of age validation methods. J. Fish Biol. *59(2),* 197–
626 242. https://doi.org/10.1111/j.1095-8649.2001.tb00127.x
627 33. Von Bertalanffy, L. (1938). A quantitative theory of organic growth (Inquiries on growth
628 laws II). Hum. Biol. *10*, 181-213.

629 34. Gompertz, B. (1825). On the nature of the function expressive of the law of human
630 mortality and on a new mode of determining the value of life contingencies. Philos. Trans. R.
631 Soc. Lond. *115*, 515–585. https://doi.org/10.1098/rspl.1815.0271.
632 35. Verhulst, P. F. (1838). Notice sur la loi que la population poursuit dans son accroissement.
633 Corresp. Math. Phys. *10***,** 113-121. http://dx.doi.org/10.1371/journal.pbio.1001827

634 36. Pauly, D. (1979). Gill size and temperature as governing factors in fish growth: a
635 generalization of von Bertalanffy's growth formula. PhD Thesis, Univ. Kiel and Institut für
636 Meereskunde.

637 37. Akaike, H. (1974). A new look at the statistical model identification. IEEE Trans. Autom.
638 Control. *19*, 716-723. http://dx.doi.org/10.1109/TAC.1974.1100705

639 38. Sakamo, Y., Ishiguro, M., and Kitagawa, G. (1986). Akaike Information Criterion
640 Statistics (Netherlands : Springer).

641 39. Boettiger, C., Lang D. T., and Wainwright, P. C. (2012). rfishbase: exploring,
642 manipulating and visualizing FishBase data from R. J. Fish Biol. *81*, 2030-2039. DOI:
643 10.1111/j.1095-8649.2012.03464.x

644 409. Chessel, D., Dufour, A., and Thioulouse, J. (2004). The ade4 Package - I: One-Table
645 Methods. R News, *4(1),* 5-10. https://cran.r-project.org/doc/Rnews/

646 41. Wickham, H. (2016). ggplot2: Elegant Graphics for Data Analysis (New York : Springer-
647 Verlag).

648 42. Kassambara, A., and Mundt, F. (2020). factoextra: Extract and Visualize the Results of
649 Multivariate Data Analyses. R package version 1.0.7. https://CRAN.R-
650 project.org/package=factoextra.

651 43. Kassambara, A. (2020). ggpubr: 'ggplot2' Based Publication Ready Plots. R package
652 version 0.4.0. https://CRAN.R-project.org/package=ggpubr.

653

654

655

A

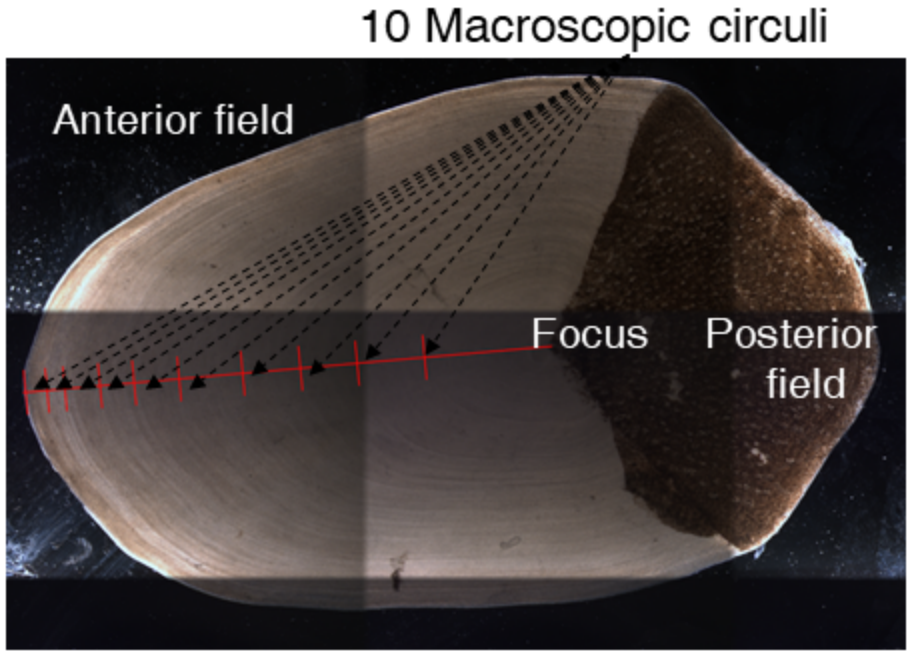
10 Macroscopic circuli
Anterior field
Focus
Posterior field

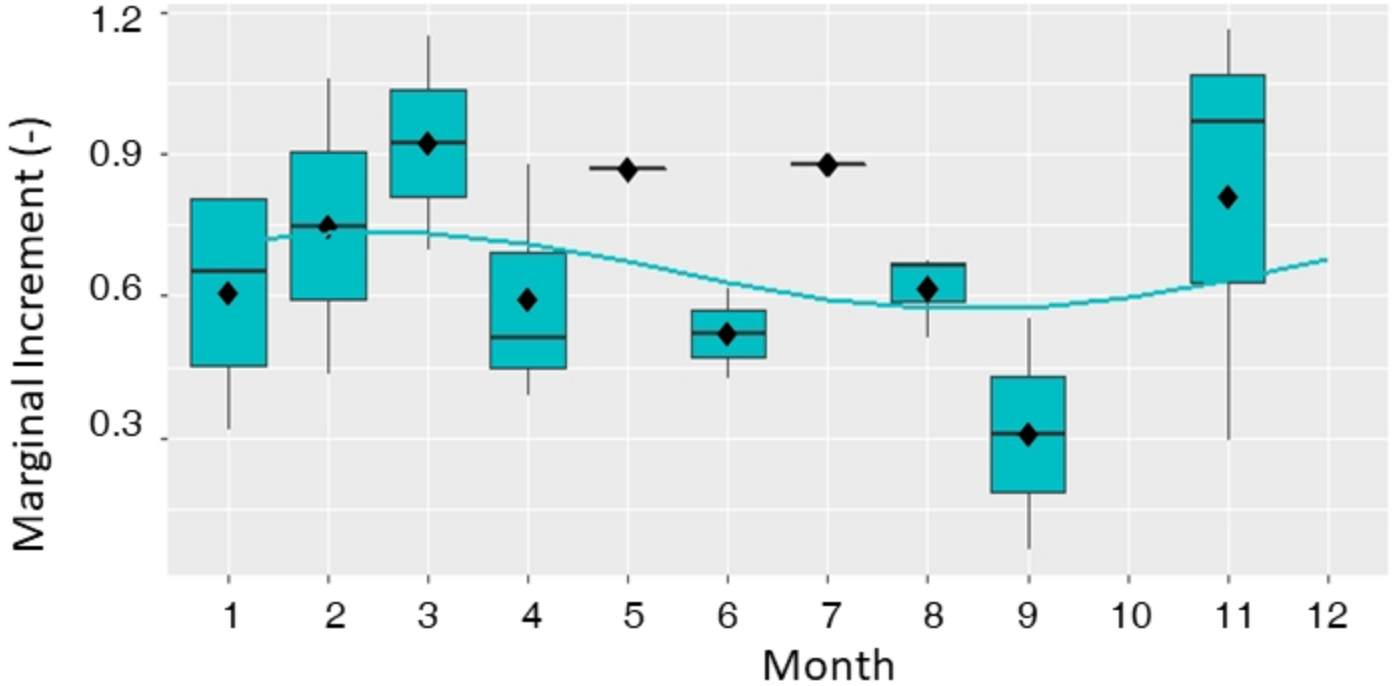
Marginal Increment (-)
1.2
0.9
0.6
0.3
1
2
3
4
5
6
7
8
9
10
11
12
Month

B

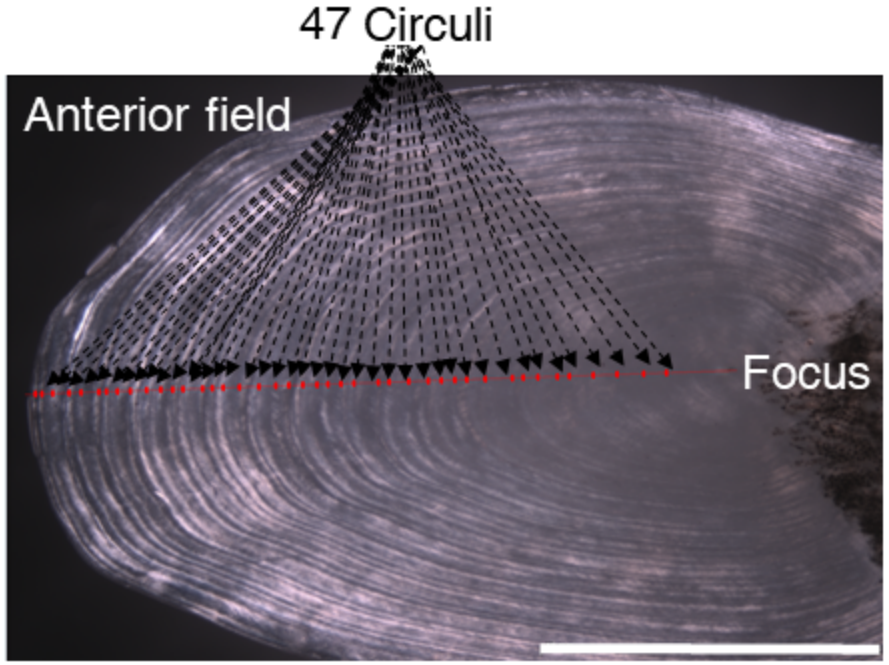
47 Circuli
Anterior field
Focus

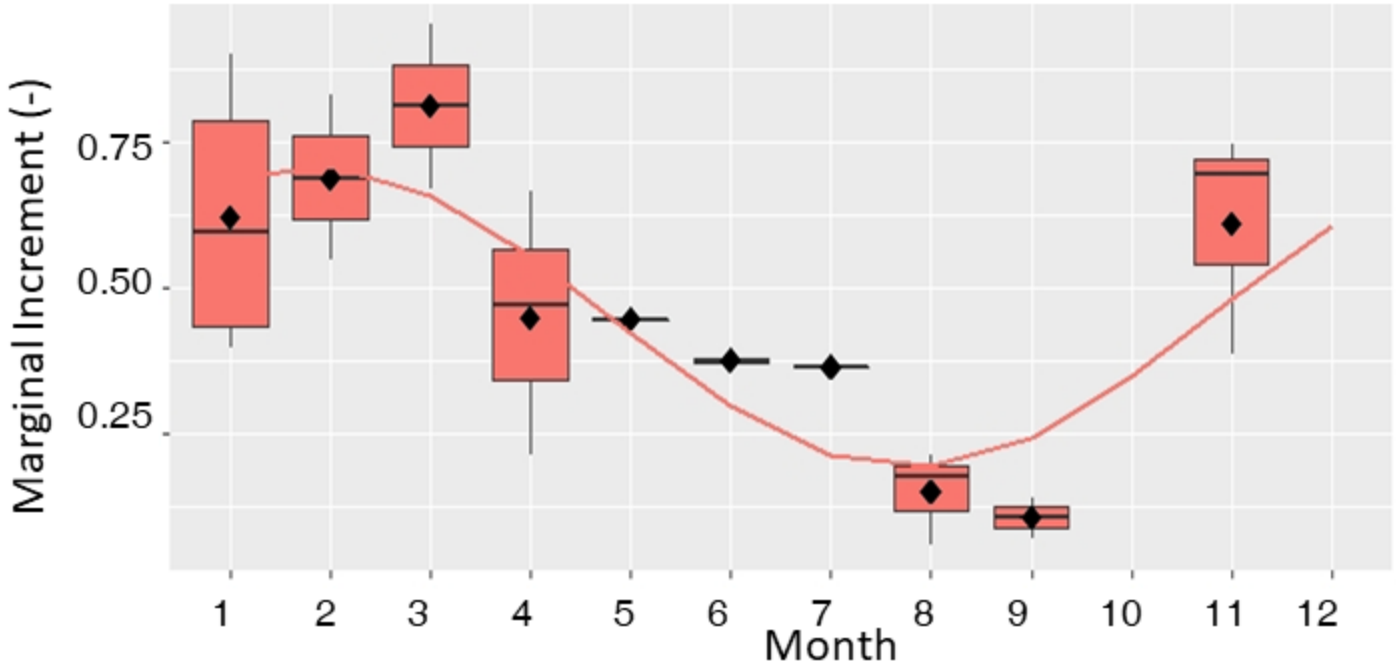
Marginal Increment (-)
0.75
0.50
0.25
1
2
3
4
5
6
7
8
9
10
11
12
Month

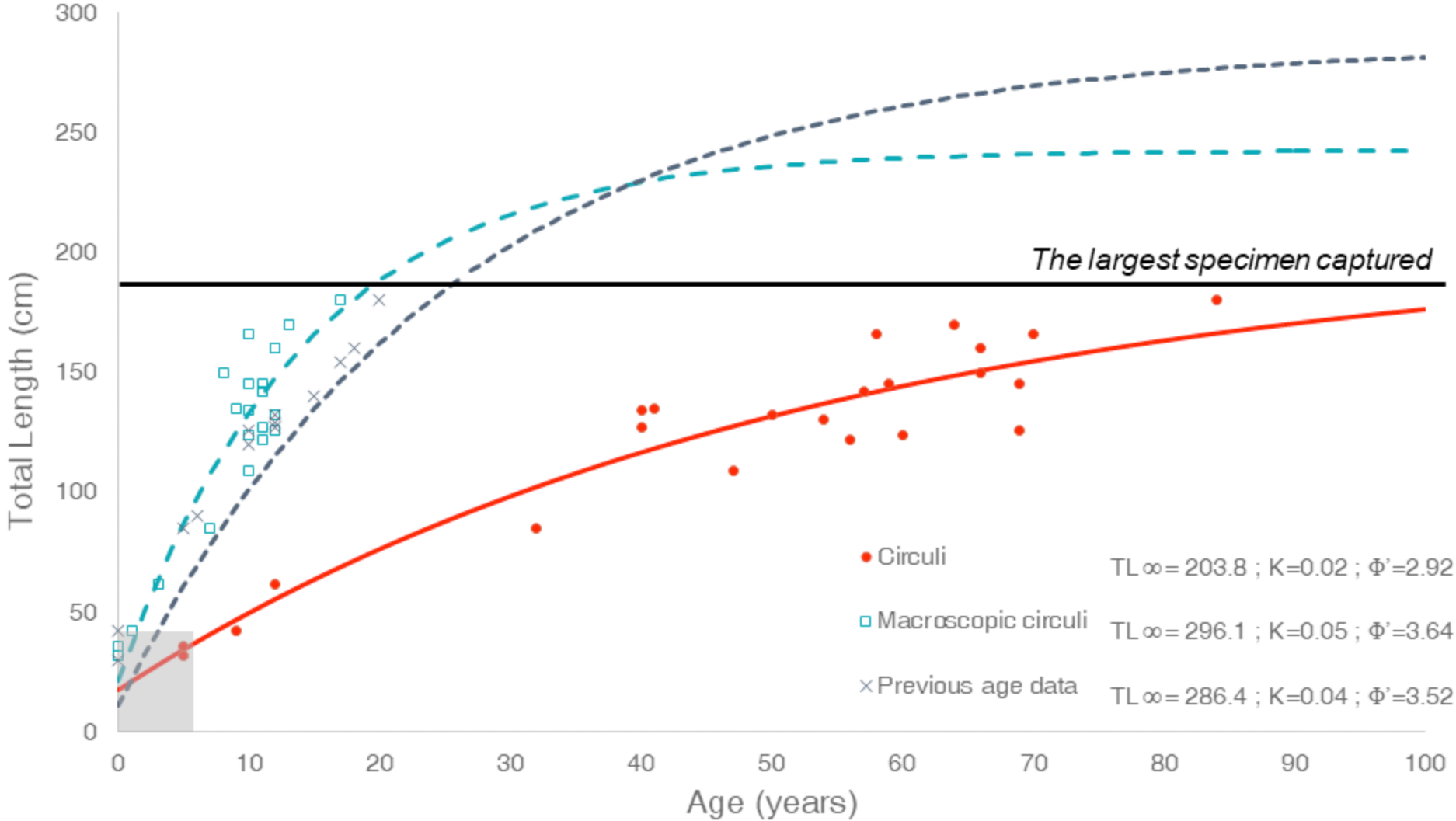
300
250
200
150
100
50
0
Total Length (cm)
0
10
20
30
40
50
60
70
80
90
100
Age (years)
The largest specimen captured
Circuli
Macroscopic circuli
Previous age data
TL∞= 203.8 ; K=0.02 ; Φ'=2.92
TL∞= 296.1 ; K=0.05 ; Φ'=3.64
TL∞= 286.4 ; K=0.04 ; Φ'=3.52

A

$\phi' = 2$ $\phi' = 3$ $\phi' = 4$ $\phi' = 5$ $\phi' = 6$ $\phi' = 7$

$\phi' = 1$

$\phi' = 0$

Growth rate coefficient, K ($year^{-1}$)

10^{1} 10^{0} 10^{-1} 10^{-2}

Coelacanth macrocirculi
Coelacanth previous study
Coelacanth circuli

10^{1} 10^{2} 10^{3}

Asymptotic total length, TL_∞ (cm)

Taxonomic group
- Coelacanth circuli
- Coelacanth macrocirculi
- Coelacanth previous study
- Deep−sea sharks
- Other species
- Roughies
- Tunas

B

Taxonomic group

Tunas
Roughies
Other species
Deep−sea sharks

64% 92% 94%

1 2 3 4 5

Growth index, $\phi' = \log_{10}(K) + 2\log_{10}(TL_\infty)$

A

B

Taxonomic group
- Coelacanth circuli
- Coelacanth macrocirculi
- Coelacanth previous study
- Deep−sea sharks
- Other species
- Roughies
- Tunas

PC2 (24.4%)

PC1 (54.5%)

Spawning frequency

Longevity

Maturation age

Growth coefficient

Coelacanth previous study

Coelacanth macrocirculi

Coelacanth circuli

Taxonomic group

Tunas

Roughies

Other species

Deep−sea sharks

0%

13%

26%

Slow−fast life−history axis, PC1

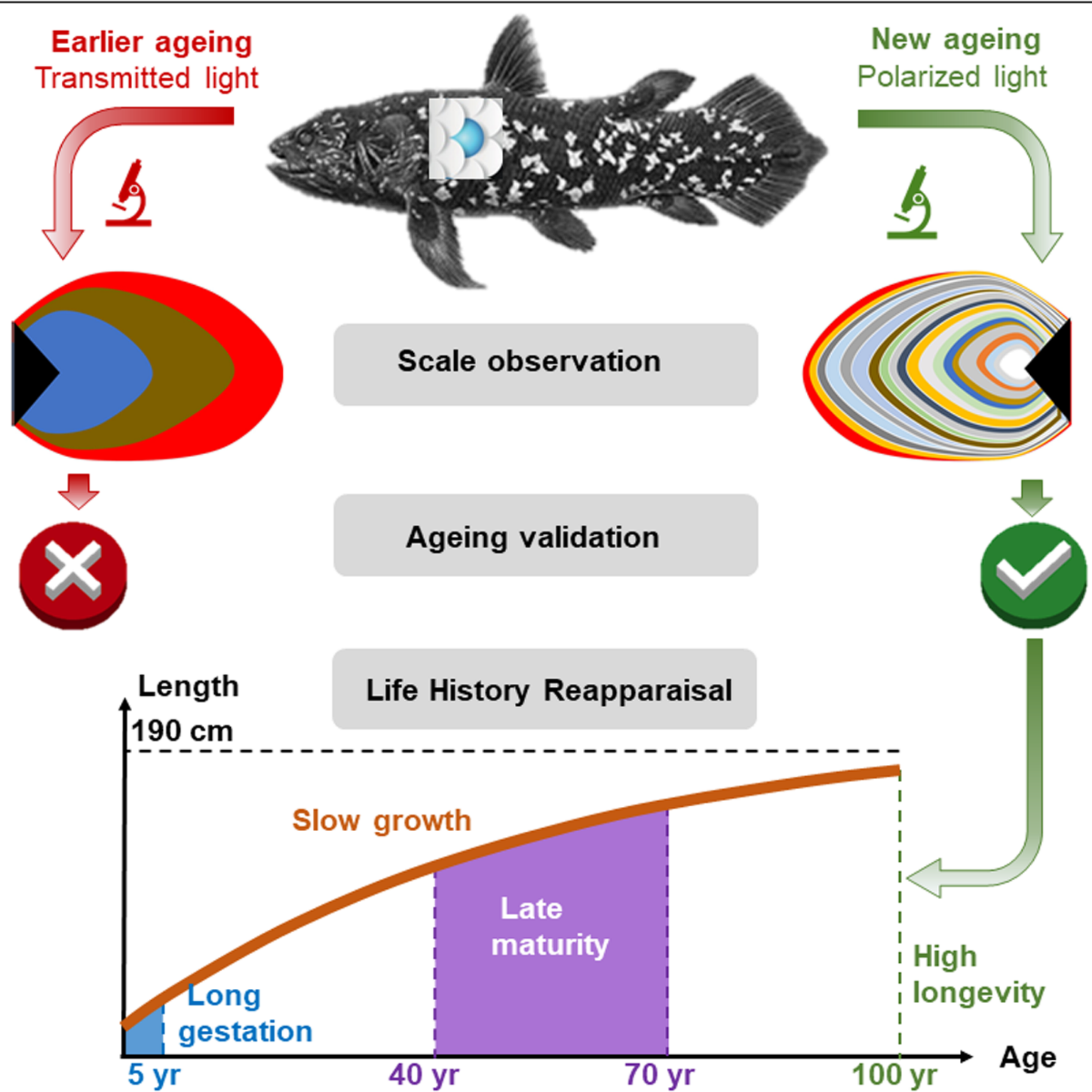
Earlier ageing
Transmitted light
New ageing
Polarized light
Scale observation
Ageing validation
Life History Reapparaisal
Length
190 cm
Slow growth
Late maturity
Long gestation
High longevity
5 yr
40 yr
70 yr
100 yr
Age